

Piezoelectric characterization and thermal stability of a high-performance α -quartz-type material, gallium arsenate

Olivier Cambon,^{a)} Julien Haines, and Guillaume Fraysse

Laboratoire de Physicochimie de la Matière Condensée, Unité Mixte de Recherche (UMR-CNRS) 5617, Université Montpellier II, cc003, Place E. Bataillon, F-34095 Montpellier, Cedex 5, France

Jacques Détaint and Bernard Capelle

Laboratoire de Minéralogie et de Cristallographie de Paris, Université Paris VI, Place Jussieu, 75252 Paris, France

Arie Van der Lee

Institut Européen des Membranes de Montpellier, Unité Mixte de Recherche-Centre National de la Recherche Scientifique (UMR-CNRS) 5635, Université Montpellier II, cc 047, 300 Avenue Professor E. Jeanbrau, F-34095 Montpellier, Cedex 5, France

(Received 28 June 2004; accepted 28 January 2005; published online 28 March 2005)

Piezoelectric measurements were performed on large single crystals (8 mm along the c direction) of an α -quartz-type piezoelectric material, gallium arsenate, GaAsO_4 , which allow us to extend the structure-property relationships in the α -quartz-type materials. These first measurements on Y -rotated-cut plates have shown that gallium arsenate is the highest-performance piezoelectric material of this group. As compared to the coupling coefficients of the other materials with the same structure ($k_{\text{SiO}_2}=8\%$, $k_{\text{AlPO}_4}=11\%$, and $k_{\text{GaPO}_4}=16\%$), gallium arsenate exhibits the highest piezoelectric coupling coefficient of about 22%, as has been predicted by the structure-property relationships. Moreover, from these piezoelectric measurements, the C'_{66} elastic constant was determined and compared with elastic constants in quartz-type materials. The proposed value for the cut angle of the AT plane in GaAsO_4 is -6.3° . In order to extend the previous thermal stability results, thermal gravimetric analysis (TGA) and x-ray diffraction have been carried out on GaAsO_4 powder at high temperatures. It has been shown that GaAsO_4 is stable up to 1030 °C. The thermal-expansion coefficient of GaAsO_4 is $4.0 \times 10^{-5} \text{ K}^{-1}$. The thermal expansion of the predicted AT plane ($Y-6.3^\circ$) in GaAsO_4 is shown to be similar to that of the other materials. Finally, it is demonstrated that the intertetrahedral bridging angle θ ($A-O-B$) of GaAsO_4 is the most stable in α -quartz materials, which enables one to predict that GaAsO_4 should retain high piezoelectric performances up to 925 °C. © 2005 American Institute of Physics. [DOI: 10.1063/1.1874293]

I. INTRODUCTION

Over the past decades, many studies have been carried out to develop piezoelectric materials,¹⁻¹⁰ with better properties than those of the most used material, α quartz. The candidate materials are principally AO_2 and ABO_4 ($A=\text{Si, Ge, Al, Ga}$ and $B=\text{P, As}$) compounds. All these materials crystallize in the $P3_121$ (or $P3_221$) space group with three formula units per cell. The structure type adopted by ABO_4 compounds is a cation-ordered derivative of the α -quartz-type structure with a doubled c parameter with respect to that of the AO_2 -type materials.

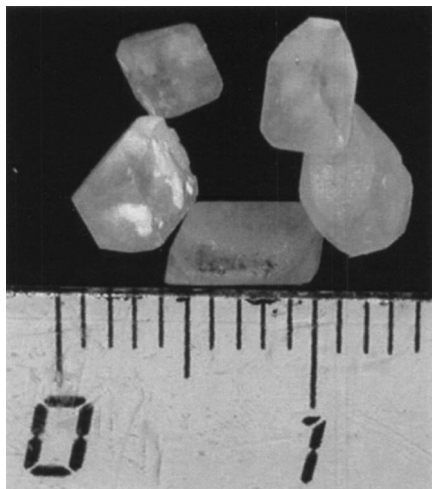
Structure-property relationships have been developed for these materials.¹¹⁻¹⁶ The evolution of various physical, elastic, thermal, dielectric, and piezoelectric properties has been determined in terms of the crystal structure of the various compounds. In the case of α quartz, the piezoelectric properties degrade beginning above 300 °C, well before the α - β transition at 573 °C.¹⁷ In contrast, based on these relationships, the most distorted structures could be expected to give rise to the highest-performance materials. Indeed, the most

distorted materials, such as GeO_2 and GaAsO_4 , for which the intertetrahedral $A-O-B$ bridging angle θ and the tilt angle δ (tetrahedral tilt angle with respect to the β -quartz structure) are, respectively, 130° and 25.7° for GeO_2 and 129.6° and 26.9° for GaAsO_4 are predicted to exhibit a high piezoelectric coupling coefficient ($k=22\%$) and to have a very high degree of thermal stability.¹³

Large single crystals of GaAsO_4 (8 mm along c axis) have been synthesized by hydrothermal methods. X and Z plates were prepared in order to measure dielectric constants ϵ'_{11} and ϵ'_{33} .¹⁸ The obtained values ($\epsilon'_{11}=8.5$ and $\epsilon'_{33}=8.6$) are the highest measured for α -quartz-type materials. The linear variation¹⁸ established between ϵ'_{11} and the coupling coefficient k can be used to predict the high piezoelectric properties for GaAsO_4 and particularly a coupling coefficient of about 22%. Up to now, no piezoelectric measurements have been performed on this material.

In the first part of this paper, the results obtained on Y -rotated cut crystals are presented. The cut angle is very close to the value predicted from structure-property relationships. The structural quality was checked by x-ray topographic methods and piezoelectric measurements were performed on these Y -rotated plates. The first piezoelectric

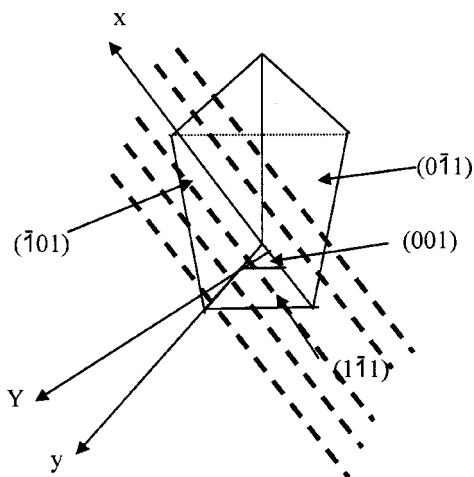
^{a)}Author to whom correspondence should be addressed; electronic mail: ocambon@lpmc.univ-montp2.fr

FIG. 1. GaAsO₄ single crystals.

measurements on GaAsO₄ are presented and the results are used to extend the structure-property relationships in α -quartz-type materials. In the second part, the thermal stability of GaAsO₄ is investigated *in situ* by thermal gravimetric analysis (TGA) and x-ray diffraction on powder samples. Finally, α -quartz-type materials are compared in terms of piezoelectric properties and thermal stability to define their field of application.

II. EXPERIMENT

Gallium arsenate crystals and powder were prepared by a hydrothermal method in a polytetrafluorethylene (PTFE)-lined autoclave as described previously.¹⁸ The faces of a selected crystal were indexed by x-ray diffraction using an Enraf-Nonius CAD4 diffractometer. The crystal was cut with a Well 4240 single-wire saw. The geometry of the crystal leads us to study only one direction, a *Y*-rotated cut (belonging to the IEEE orthogonal references¹⁹). The cut angle was checked by x-ray diffraction with the diffractometer described above. In order to improve the piezoelectric response of the samples, the thickness of the plates was reduced by polishing.

FIG. 2. Orientation of the *Y*-rotated-cut plates.

X-ray topography was used to check the structural quality of the GaAsO₄ crystal. This method corresponds to a Laue experiment. Due to the very high x-ray absorption of GaAsO₄, synchrotron radiation of DCI ring (LURE, Orsay) was used. Each lattice plane is in diffraction condition for one wavelength and its harmonics in the white spectrum, which allows us to obtain one image of the crystal for each diffraction vector. Dark contrasts on the obtained photo are due to structural defects such as dislocations, twins, or inclusions.

Piezoelectric measurements were performed by the air-gap method with nonadherent electrodes on the plates. The air-gap setup used for these measurements²⁰ can provide air gaps varying from zero to several tens of microns with an absolute accuracy and a reproducibility of 1 or 2 μm . Gaps smaller than this can also be obtained by detecting the contact of the probe with the sample based on the onset of a larger attenuation and the change of the response. In the present study, as small gaps as possible (a few microns) have been chosen while avoiding the contact between the probe and the sample. The upper electrode was a 5-mm-diameter rod of Invar with a polished flat face and the lower electrode a gold thin film deposited on a flat piece of polished silica. A Hewlett-Packard (HP) network analyzer was used to measure the piezoelectric performances (resonance F_r and antiresonance F_a frequencies and coupling coefficient k). The thickness of the plates was measured by a micrometer with an accuracy of $\pm 1 \mu\text{m}$.

In order to investigate the thermal stability of GaAsO₄, TGA was performed up to 1250 °C using a Setaram Labsys instrument. 190.1 mg of GaAsO₄ powder were introduced into a platinum crucible. The heating rate was 5°/mn. The signal of the crucible was subtracted from the experimental results.

High-temperature x-ray powder-diffraction measurements were performed on a PANanalytical X'Pert diffractometer equipped with an X'Celerator detector using Ni-filtered, Cu K α radiation. GaAsO₄ powder, which had been ground and passed through a 20- μm sieve followed by annealing at 800 °C (to eliminate the hydrated compounds eventually present in the powder), was placed in the sample holder of an Anton Paar HTK 1200 high-temperature oven chamber. X-ray diffraction data were obtained over the 19°–

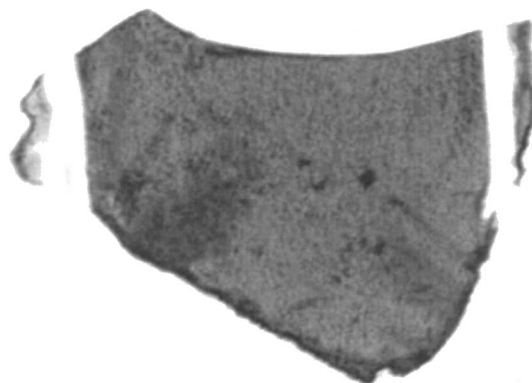
FIG. 3. X-ray topography of a *Y*-rotated plate of GaAsO₄. (The two white bars at the extremities of the sample are due to the supports.)

TABLE I. Air-gap piezoelectric results.

Third or fifth overtone (MHz)	Fundamental mode (MHz)	Overtone order (n)	k (%)	Wave velocity (m/s)	C'_{66} (GPa)
Sample1					
$(d=0.195 \text{ mm})$					
16.690 39	5.435 84	3.0704	25.65	2176	18.8
16.691 46	5.435 84	3.0706	25.69	2176	18.8
16.690 39	5.460	3.0568	23.02	2175	19.0
16.691 46	5.460	3.057	23.06	2175	19.0
Sample2					
$(d=0.194 \text{ mm})$					
16.833 62	5.519 65	3.0498	21.53	2182	19.2
16.834 57	5.519 65	3.0499	21.57	2182	19.2
16.833 62	5.533 01	3.0424	19.86	2181	19.4
16.834 57	5.533 01	3.0426	19.90	2181	19.4
16.833 62	5.552 47	3.0317	17.17	2180	19.5
16.834 57	5.552 47	3.0319	17.22	2180	19.5
28.009 06	5.519 65	5.0744	19.62	2175	19.3
28.0018	5.519 65	5.0731	19.45	2174	19.3
28.009 06	5.533 01	5.0622	17.93	2175	19.4
28.0018	5.533 01	5.0609	17.74	2174	19.4
Sample3					
$(d=0.189 \text{ mm})$					
17.062 25	5.611 61	3.0405	19.42	2153	18.9
17.065 06	5.611 61	3.041	19.54	2154	18.9
17.068 01	5.611 61	3.0416	19.66	2154	18.9
Average			20.47	2173	19.2

124° range in 2θ over the temperature range up to 925°C . Acquisition times were approximately 3 h. Rietveld refinements were performed with the program FULLPROF.²¹ Due to the relatively low scattering factor of oxygen, soft constraints were applied to the Ga–O and As–O distances.

III. RESULTS AND DISCUSSION

A. Y-rotated cut plates

After growing GaAsO_4 crystals,¹⁸ their faces were indexed by x-ray diffraction (Fig. 1) and Y-rotated-cut plates were sawn (Fig. 2). A Y-rotated cut is a plate whose surface is parallel to the crystallographic x axis and produces an angle (termed cut angle) with the z axis. Structure-property relationships²² show that the angle for an AT cut (athermal cut: lowest variation of the resonance frequency with tem-

perature) for GaAsO_4 should be -5° . This value was selected to cut the crystal. After cutting, the orientation of the plates was checked by x-ray diffraction. The plane of the plates is (041) , which corresponds to a cut angle of -6.26° which is in the same range as the target value of -5° .

X-ray topography (Fig. 3) of the plates indicates the high structural quality of the raw material that is necessary to undertake very accurate piezoelectric measurements. Only a few contrasts indicate the presence of certain defects. The black point in the middle of the photo probably corresponds to a solvent inclusion. The general aspect of the plate is due to the surface state of the plate which is not of optical quality.

B. Piezoelectric characterizations

1. Air-gap measurements

In the air-gap measurements, complex responses were observed for the fundamental mode for nearly all the samples, which display many resonances between the expected resonance frequency of the thickness shear mode and a frequency slightly above the expected antiresonance frequency. This kind of response is due to the coupling of the thickness shear with several plate modes most probably due to the boundary conditions at the edge of the plate. The response for the third overtone was generally more conventional with less modes and often several resonances very close to the strongest. The fifth overtone was generally weak with one or two resonances. No resonance that can be definitively assigned to the seventh overtone was observed in any sample. The first resonance frequencies observed for two samples are given in Table I. In this table, the results given

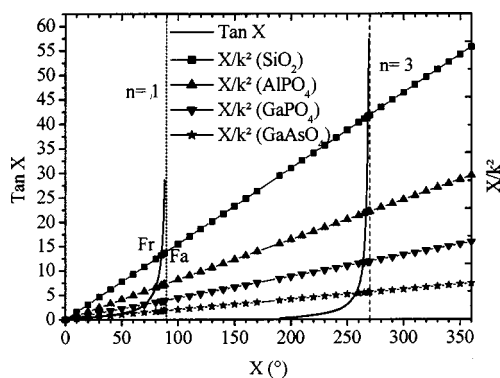


FIG. 4. Graphical resolution of $\tan X = X/k^2$ with $X = n\pi\omega_r/2\omega_a$ for the four well-known α -quartz-type materials.

TABLE II. AT-cut characteristic parameters of the well-characterized α -quartz materials compared to the corresponding experimental values obtained for GaAsO₄.

Material	SiO ₂ (Ref. 32)	AlPO ₄ (Ref. 5)	GaPO ₄ (Refs. 33and34)	GaAsO ₄
AT-cut angle (°)	-35.15	-33.02	-15.9	-6.3
Cristallographic plane for AT cut	(012)	(047)	(043)	(041)
A-O-B angle (°)	143.2	142.4	134.2	129.6
Coupling coefficient k (%)	8	11	16	21-23
C_{66} (GPa)	40	29.4	22.38	
C_{11} (GPa)	86.79	69.3	66.58	
C_{12} (GPa)	6.79	10.5	21.81	
C_{13} (GPa)	12.01	13.5	24.87	
C_{33} (GPa)	105.79	88.6	102.1	
C_{44} (GPa)	58.21	43	37.66	
C_{14} (GPa)	18.12	13	3.91	
C_{66} (GPa)	28.9	21.6	21.3	19.2
Density (g/cm ³)	2.64	2.63	3.57	4.23
AT-cut wave velocity (m/s)	3307	2863	2442	2173

for the samples 1 and 2 were obtained with the same plate (as polished for the sample 1, and slightly etched for the sample 2).

The calculations were made using the one-dimensional model for thickness shear.^{23,24} This model, in which in the present case one thickness mode is excited, leads to the following expression of the electrical impedance of the resonator:

$$Z(\omega_r) = \frac{1}{j\omega_r C_0} \left(1 - k^2 \frac{\tan X}{X} \right) \text{ with } X = \frac{n\pi\omega_r}{2\omega_a}, \quad (1)$$

where k is the coupling coefficient of the mode, C_0 the static capacity, ω_r is the resonance frequency of the n th overtone, ω_a is the antiresonance frequency of the n th overtone, and n is the order of the overtone (n is an odd number).

At any resonance frequency of any overtone (n): $Z(\omega_r)=0$ and $\tan X=X/k^2$

$$X = \frac{n\pi\omega_r}{2\omega_a} = \frac{\omega_r d}{2V} \text{ with } V = \omega_a \frac{d}{n\pi} = \sqrt{\frac{C}{\rho}} \quad (2)$$

and

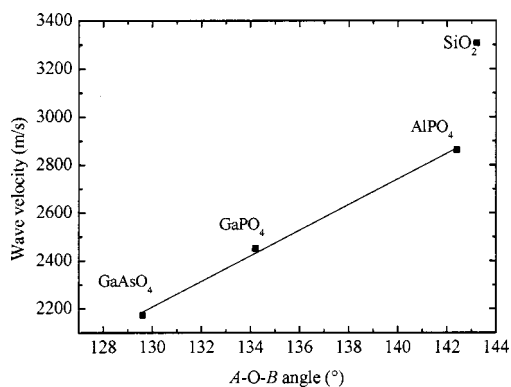


FIG. 5. Wave velocity of the shear mode vibration (associated with the C'_{66} elastic constant) of the AT cut in the α -quartz materials.

$$\omega_a = \omega_r \left(\frac{4k^2}{n^2\pi^2} + 1 \right), \quad (3)$$

where V is the wave velocity, d the thickness of the plate, and ρ the density (4.23 g/cm³ for GaAsO₄).

C is the stiffened elastic constant of the shear mode. In order to take into account the piezoelectric effect, a correction²⁵ has to be applied using the following equation:

$$C = \bar{C}(1 - k^2). \quad (4)$$

After this correction, the elastic constant C (element of the Christoffel matrix) refers to constant D and is comparable to the value obtained by conventional methods such as Brillouin scattering or pulse echo measurements.

The principle of the calculation is to take for each sample one resonance of an overtone (n) and one resonance of the fundamental mode to compute the ratio of their frequencies. For the “true” thickness shear mode, this ratio should be greater than n due to the properties of the roots of the $Z(\omega)=0$ equation (since $k < 1$). If this is the case, with graphical resolution (Fig. 4) and considering the previous equations it is possible to solve simultaneously the $Z(\omega)=0$ equation for the two modes and extract the coupling coefficient k , the wave velocity V , and consequently the elastic

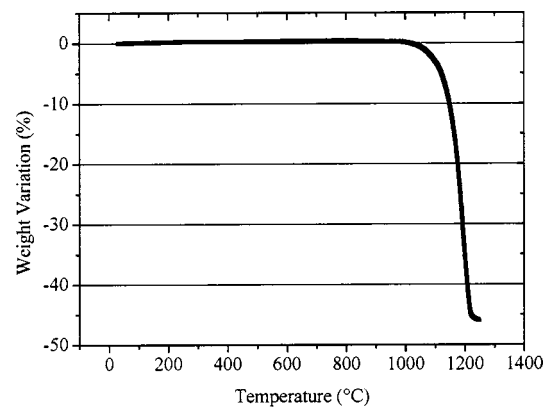


FIG. 6. TGA measurements on GaAsO₄ powder.

TABLE III. Unit-cell parameters, volume, and agreement factors for GaAsO₄ as a function of temperature.

T (°C)	a (Å)	c (Å)	V (Å ³)	R_p	R_{wp}	R_B
25	4.997(1)	11.386(1)	246.2(1)	30.7	17.3	9.98
200	5.011(1)	11.393(1)	247.7(1)	32.1	17.5	11.4
400	5.029(1)	11.402(1)	249.7(1)	32.9	17.4	10.7
600	5.047(1)	11.411(1)	251.7(1)	33.2	17.0	10.5
800	5.065(1)	11.419(1)	253.7(1)	34.6	17.3	10.1
850	5.069(1)	11.421(1)	254.2(1)	36.1	17.6	11.1
925	5.077(1)	11.425(1)	255.0(1)	36.2	17.5	10.9

constant \bar{C} of the considered thickness shear mode. It can be observed on Fig. 4 that the gap between Fr and Fa increases with high electromechanically coupled materials such as GaAsO₄. This property is often required for large band piezoelectric filters, for example. The elastic constants measured under piezoelectric excitation are corrected as above. In the present case, the samples are Y -rotated cuts for which the elastic constant termed C'_{66} is calculated from the previous Eqs. (2) and (4) and is related to the cut angle θ by the following relationship:

$$C'_{66} = C_{44} \sin^2 \theta + C_{66} \cos^2 \theta + 2C_{14} \cos \theta \sin \theta. \quad (5)$$

These calculations were performed for all measured modes near the expected fundamental resonance of the thickness shear mode and of its overtones (Table I). These results indicate that gallium arsenate has the highest coupling coefficient among all known quartz analogs and the lowest wave velocity. Some scatter is observed certainly due to differences in the material (impurities or solvent inclusions) of these samples. The lowest values tend to underestimate the average coupling coefficient, whose value can reach 22% or 23%.

The average values show, from the point of view of piezoelectric properties, that GaAsO₄, as was predicted, is a promising material with a high coupling coefficient. It must be noted that these first measurements have been made using the air-gap method. Thus, the piezoelectric values and particularly the Q value (quality factor) can be increased by manufacturing conventional resonators with adherent thin-film electrodes. The C'_{66} value obtained from the present measurements is 19.2 ± 0.2 GPa.

2. Comparison to the other α -quartz-type materials

In previous studies,^{11–16} many authors have established different relationships between the structural distortion and

the piezoelectric properties in α -quartz-type materials. Based on these results, it was predicted that GaAsO₄ should be an excellent piezoelectric material²² with high coupling coefficient (22%) for an AT-cut angle near -5° . These first experimental results on $Y-6.3^\circ$ -rotated cut confirm this prediction. The coupling coefficient of GaAsO₄ is found to be almost 50% greater than that of GaPO₄ (Table II), until now the most highly coupled material of this material family.

From the elastic constants and the well-known AT-cut angle θ of the α -quartz materials, C'_{66} values are determined and the wave velocity of the AT cut is compared to the experimental value found in the case of GaAsO₄ (Table II). If it is reasonable to consider a linear variation of the wave velocity values in terms of distortion in the ABO₄ materials (Fig. 5), the experimental value of 2173 m/s fits very well, which confirms the value of 19.2 GPa for the C'_{66} constant of GaAsO₄. Moreover, this result confirms that the AT-cut angle should be near this experimental value of -6.3° . It must be noted that AO₂ materials (i.e., SiO₂) are not included in this linear variation because this type of material is built up of only one type of tetrahedron AO₄.

C. Thermal behavior

1. Thermal analysis

TGA results (Fig. 6) up to 1250 °C indicate the beginning of the weight loss at 1030 °C which reaches 46% at the end of the run. This weight loss corresponds to the thermal decomposition of GaAsO₄ following the reaction:



X-ray diffraction measurements performed on a powder before and after TGA analysis confirm this reaction. No presence of As₂O₅ is found in the recovered Ga₂O₃ compound because As₂O₅ is not stable and sublimes at 315 °C.^{26,27}

TABLE IV. Fractional atomic coordinates and isotropic atomic displacement parameters (Å²) of GaAsO₄ as a function of temperature. Trigonal: $P3_121$ $Z=3$, Ga: $3a$ sites ($x,0,1/3$), As: $3b$ sites ($x,0,5/6$), O: $6c$ sites (x,y,z).

T (°C)	x (Ga)	x (As)	B_{iso} (Ga,As)	$x(\text{O}_1)$	$y(\text{O}_1)$	$z(\text{O}_1)$	$x(\text{O}_2)$	$y(\text{O}_2)$	$z(\text{O}_2)$	$B_{\text{iso}}(\text{O}_1, \text{O}_2)$
25	0.4519(1)	0.4520(2)	2.50(2)	0.3855(12)	0.3043(14)	0.3888(5)	0.4027(17)	0.2926(13)	0.8729(4)	3.30(13)
200	0.4528(1)	0.4543(2)	3.06(3)	0.3835(15)	0.3010(14)	0.3893(5)	0.4015(16)	0.2889(13)	0.8740(4)	2.97(13)
400	0.4541(1)	0.4563(2)	3.51(3)	0.3822(14)	0.2975(13)	0.3900(5)	0.3961(15)	0.2817(13)	0.8761(4)	3.52(13)
600	0.4550(1)	0.4578(2)	3.75(3)	0.3838(14)	0.2967(13)	0.3900(5)	0.4039(16)	0.2854(13)	0.8750(4)	4.26(14)
800	0.4556(1)	0.4590(2)	4.03(3)	0.3877(16)	0.2982(14)	0.3893(5)	0.4007(16)	0.2805(13)	0.8767(4)	4.45(14)
850	0.4559(1)	0.4589(2)	3.97(3)	0.3935(18)	0.3027(16)	0.3880(6)	0.4034(19)	0.2830(15)	0.8760(5)	5.77(16)
925	0.4552(1)	0.4584(2)	4.22(3)	0.3888(16)	0.2980(14)	0.3898(5)	0.4019(16)	0.2807(13)	0.8771(4)	5.26(15)

TABLE V. Intertetrahedral Ga–O–As bridging and tetrahedral tilt angles ($^\circ$) in GaAsO₄ as a function of temperature.

T ($^\circ\text{C}$)	Ga–O ₁ –As ($^\circ$)	Ga–O ₂ –As ($^\circ$)	Ga–O–As _{average} ($^\circ$)	$\delta_{\text{av}}\text{GaO}_4$	$\delta_{\text{av}}\text{AsO}_4$	δ_{av}
25	130.5(3)	130.4(3)	130.4(3)	23.1(4)	27.5(4)	25.3(4)
200	130.6(3)	131.0(3)	130.8(3)	22.6(4)	26.9(4)	24.8(4)
400	130.9(3)	131.5(3)	131.2(1)	22.0(4)	26.0(4)	24.0(4)
600	131.4(3)	132.2(3)	131.8(3)	21.8(4)	26.1(4)	24.0(4)
800	131.9(3)	132.8(3)	132.4(3)	21.7(4)	25.4(4)	23.6(4)
850	132.2(4)	132.8(3)	132.5(4)	22.2(5)	25.6(5)	23.9(5)
925	132.4(3)	133.3(3)	132.8(3)	21.5(4)	25.2(4)	23.3(4)

2. X-ray diffraction at high temperatures

a. Structural stability. The structural refinements for temperatures up to 925 $^\circ\text{C}$ (Tables III–V) are in good agreement with and complement the previous single-crystal x-ray diffraction studies up to 800 $^\circ\text{C}$.¹³ Very good agreement was obtained between experimental and calculated profiles (Fig. 7). The present values indicate that the Ga–O–As intertetrahedral bridging angles are very stable (Fig. 8) in comparison with those of other materials. The slope of the curve integrated up to 400 $^\circ\text{C}$ is the lowest for GaAsO₄ (2.1×10^{-3} $^\circ/\text{K}$) in comparison with quartz (7.4×10^{-3} $^\circ/\text{K}$), berlinite (8.7×10^{-3} $^\circ/\text{K}$), and even GaPO₄ (5.2×10^{-3} $^\circ/\text{K}$). Thus, GaAsO₄ is the most thermally stable α -quartz material. Moreover, the variation of Ga–O–As in-

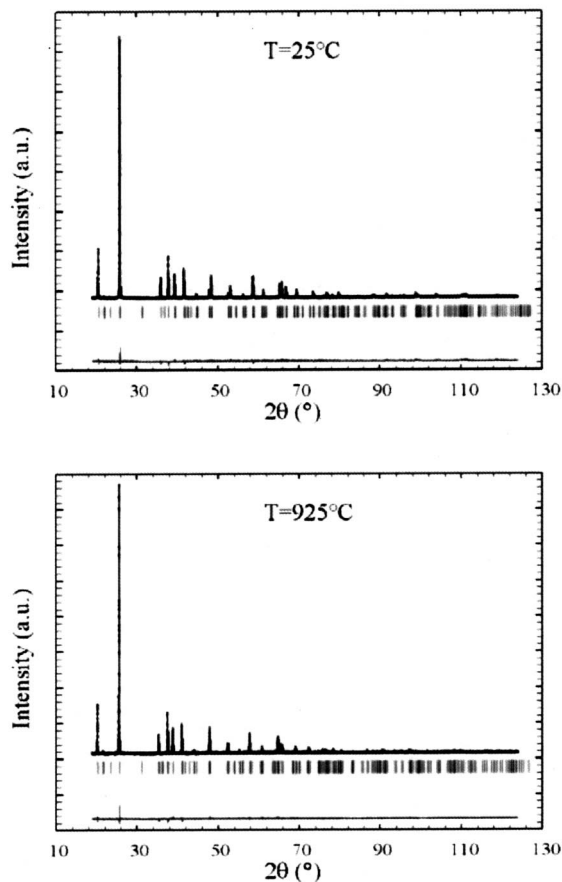


FIG. 7. Experimental (+) and calculated (solid line) powder-diffraction profiles from the Rietveld refinements of the structure of GaAsO₄. The lower curve is the difference curve between experimental and calculated profiles.

tertetrahedral bridging angles is linear up to 925 $^\circ\text{C}$, whereas the corresponding variation is linear only up to 800 $^\circ\text{C}$ for GaPO₄. This behavior leads us to conclude that the piezoelectric properties of GaAsO₄ should be stable up to at least 925 $^\circ\text{C}$, whereas the piezoelectric properties of GaPO₄ degrade beginning at 800 $^\circ\text{C}$.²⁸ Thus, for GaAsO₄ resonators, it is probably possible to increase the useful temperature range by at least 125 $^\circ$ compared to GaPO₄.

b. Thermal expansion. The temperature dependence of the cell volume was fitted with a linear function and the thermal volume expansion coefficient of GaAsO₄ normalized at 298 K is found to be $\alpha_{v(298\text{ K})} = 4.0 \times 10^{-5}$ K^{-1} . This value is in the same range as that of quartz,^{29,30} or berlinite.³¹ As for the other α -quartz materials, there is a preferential expansion along the a axis: $\alpha_{a(298\text{ K})} = 1.78 \times 10^{-5}$ and $\alpha_{c(298\text{ K})} = 3.78 \times 10^{-6}$.

It is proposed, based on the above piezoelectric results, to assign the AT-cut plane to the (041) plane for which the interplanar distance d can be calculated from the x-ray diffraction data. It is thus possible to estimate the thermal expansion of the AT plane. By comparing the $d_{(\text{AT cut})}$ at different temperatures relative to the value at room temperature, it is possible to determine the thermal-expansion coefficient for the AT plane for each material (Fig. 9). Quartz and berlinite exhibit important variations in the interplanar distance of the AT plane above 400 $^\circ\text{C}$ due to the α - β transition. Linear regressions of $d_{(\text{AT cut})}$ as a function of temperature ($T < 400$ $^\circ\text{C}$) permit the materials to be compared. GaAsO₄ presents an AT-plane thermal-expansion coefficient of

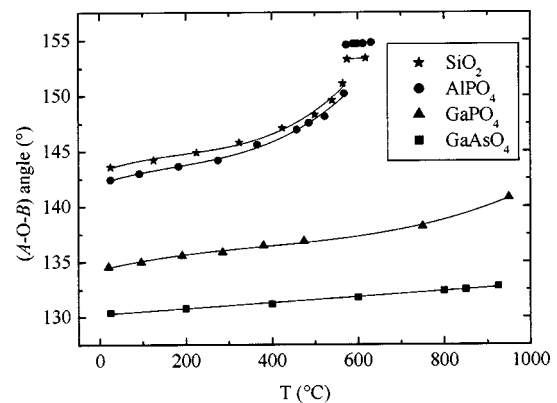


FIG. 8. Temperature dependence of the intertetrahedral (A–O–B) bridging angle in α -quartz materials (see Refs. 29, 31, 35, and 36).

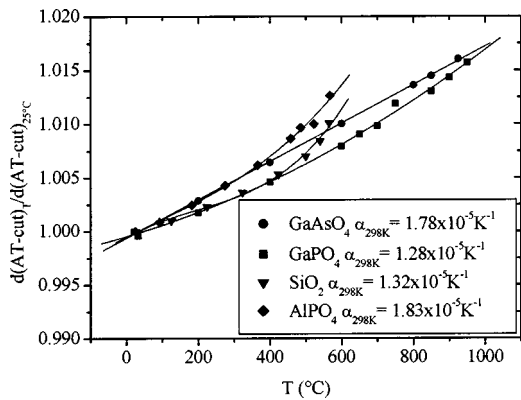


FIG. 9. Evolution of the normalized interplanar distance of the AT plane as a function of the temperature for the well-characterized α -quartz materials (see Refs. 29, 31, and 36).

$\alpha_{AT(298\text{ K})} = 1.78 \times 10^{-5} \text{ K}^{-1}$, which is the same as those of the x (or y) axis (confirmation of the cut angle, which is close to the xz plane) and essentially identical to those of berlinite ($1.83 \times 10^{-5} \text{ K}^{-1}$). GaPO_4 and quartz exhibit the lowest values of 1.28×10^{-5} and $1.32 \times 10^{-5} \text{ K}^{-1}$, respectively.

IV. CONCLUSION

The first piezoelectric measurements on gallium arsenate have been performed on ($Y\ 6.3^\circ$)-rotated-cut plates obtained from large single crystals grown by hydrothermal methods. X-ray topography indicates that the crystal is of high quality. The piezoelectric results indicate that the coupling coefficient (21.5%–23%) for the AT-cut angle is the highest among α -quartz isotypes, thereby confirming previous extrapolations based on structure-property relationships. The experimental wave velocity (2173 m/s) confirms that the AT cut is close to -6.3° . Concerning the thermal stability of GaAsO_4 , TGA results show that this compound decomposes into its constituent binary oxides above 1030 °C. Structure refinements using x-ray powder-diffraction data up to 925 °C confirm the very high stability of the fine structure of GaAsO_4 . Thus, GaAsO_4 -based resonators should work up to 925 °C (at least 125 °C higher than for GaPO_4). Moreover, the AT-cut angle has been confirmed by comparison of the thermal expansion of the AT-cut plane for the four well-characterized α -quartz-type materials.

It has thus been shown experimentally that GaAsO_4 exhibits the best piezoelectric properties and is the most thermally stable material in the α -quartz group.

¹J. P. Hou and B. H. T. Chai, Proc.-IEEE Ultrason. Symp. 419 (1987).

²E. D. Kolb and R. A. Laudise, J. Cryst. Growth **43**, 313 (1978).

³E. Philippot *et al.*, Fourth European Frequency and Time Forum (EFTF,

Neuchâtel, 1990), p. 577.

⁴J. Détaint, H. Poignant, and Y. Toudic, *Proceedings of the 34th Annual Frequency Control Symposium* (IEEE, New York, 1980), p. 93.

⁵D. S. Bailey, J. C. Andle, D. L. Lee, W. Soluch, J. F. Vetelino, and B. H. T. Chai, Proc.-IEEE Ultrason. Symp. 335 (1983).

⁶S. Hirano, K. Miwa, and S. Naka, J. Cryst. Growth **79**, 215 (1986).

⁷S. Hirano and P. C. Kim, J. Mater. Sci. **26**, 2805 (1991).

⁸P. W. Krempf, F. Krispel, and W. Wallnöffer, Ann. Chim. (Paris) **22**, 623 (1997).

⁹D. Palmier, M. Cochez, R. Gohier, C. Bonjour, G. Marianneau, A. Zarembovitch, E. Bigler, and E. Philippot, *Proceedings of the Ninth European Frequency and Time Forum* (EFTF, Besançon, 1995), p. 59.

¹⁰P. Yot, O. Cambon, D. Balitsky, A. Goiffon, E. Philippot, B. Capelle, and J. Détaint, J. Cryst. Growth **224**, 294 (2001).

¹¹E. Philippot, A. Goiffon, A. Ibanez, and M. Pintard, J. Solid State Chem. **110**, 356 (1994).

¹²E. Philippot, D. Palmier, M. Pintard, and A. Goiffon, J. Solid State Chem. **123**, 1 (1996).

¹³E. Philippot, P. Armand, P. Yot, O. Cambon, A. Goiffon, G. J. McIntyre, and P. Bordet, J. Solid State Chem. **146**, 114 (1999).

¹⁴J. Haines, C. Chateau, J. M. Léger, and R. Marchand, Ann. Chim. (Paris) **26**, 209 (2001).

¹⁵J. Haines, O. Cambon, E. Philippot, L. Chapon, and S. Hull, J. Solid State Chem. **166**, 434 (2002).

¹⁶J. Haines, O. Cambon, R. Astier, P. Fertey, and C. Chateau, Z. Kristallogr. **219**, 32 (2004).

¹⁷J. Haines, O. Cambon, D. A. Keen, M. G. Tucker, and M. T. Dove, Appl. Phys. Lett. **81**, 1 (2002).

¹⁸O. Cambon, P. Yot, S. Rul, J. Haines, and E. Philippot, Solid State Sci. **5**, 469 (2003).

¹⁹IEEE standard on piezoelectricity (IEEE, New York, NY, 1978), p. 10017.

²⁰J. Détaint, H. Carru, J. Schwartzel, A. Zarka, and B. Capelle, *Proceedings of the 43rd Annual Frequency Control Symposium* (IEEE, New York, 1989), p. 563.

²¹J. Rodriguez-Carvaja (unpublished).

²²O. Cambon and J. Haines, *Proceedings of the 2003 IEEE International Frequency Control Symposium and PDA Exhibition jointly with the 17th European Frequency and Time Forum* (IEEE, Piscataway, NJ, 2003), p. 650.

²³W. G. Cady, *Piezoelectricity: An Introduction to the Theory and Applications of Electromechanical Phenomena in Crystals*, 1964th edition (Dover Publication Inc., New York, 1964), Vol. 1–2.

²⁴J. P. Aubry, Techniques de l'Ingénieur **E1 890**, 1 (1988).

²⁵J. Détaint, J. Schwartzel, C. Joly, and E. Philippot, *Proceedings of the Third European Frequency and Time Forum* (EFTF, Besançon, 1989), p. 227.

²⁶E. C. Shafer and R. Roy, J. Am. Ceram. Soc. **39**, 330 (1956).

²⁷K. Kosten and H. Arnold, Z. Kristallogr. **152**, 119 (1980).

²⁸O. Cambon, J. Haines, G. Fraysse, and D. A. Keen, J. Phys. IV (in press).

²⁹K. Kihara, Eur. J. Mineral. **2**, 63 (1990).

³⁰M. S. Ghiorso, I. S. E. Carmichael, and L. K. Moret, Contrib. Mineral. Petrol. **68**, 307 (1979).

³¹Y. Maruoka and K. Kihara, Phys. Chem. Miner. **24**, 243 (1997).

³²B. J. James, *Proceedings of the 42nd Annual Frequency Control Symposium* (IEEE, New York, 1988), p. 146.

³³W. Wallnöffer, P. W. Krempf, and A. Asenbaum, Phys. Rev. B **49**, 10075 (1993).

³⁴P. W. Krempf, Proc.-IEEE Ultrason. Symp. 949 (1994).

³⁵H. Nakae, K. Kihara, M. Okuno, and S. Hirano, Z. Kristallogr. **210**, 746 (1995).

³⁶J. Haines, O. Cambon, N. Prudhomme, D. A. Keen, L. Chapon, and M. G. Tucker (unpublished).